HHS Public Access

Author manuscript

Transfusion. Author manuscript; available in PMC 2017 April 01.

Published in final edited form as:

Transfusion. 2016 April ; 56(4): 844–851. doi:10.1111/trf.13449.

Shape matters: the effect of red blood cell shape on perfusion of an artificial microvascular network

Nathaniel Z. Piety[a], **Walter H. Reinhart**[b], **Patrick H. Pourreau**[a], **Rajaa Abidi**[a], and **Sergey S. Shevkoplyas**[a,*]

[a]Department of Biomedical Engineering, Cullen College of Engineering, University of Houston, Houston, Texas, United States of America [b]Department of Internal Medicine, Kantonsspital Graubünden, Chur, Switzerland

Abstract

BACKGROUND—The shape of human red blood cells (RBCs) deteriorates progressively throughout hypothermic storage, with echinocytosis being the most prevalent pathway of this morphological lesion. As a result, each unit of stored blood contains a heterogeneous mixture of cells in various stages of echinocytosis and normal discocytes. Here we studied how the change in shape of RBCs following along the path of the echinocytic transformation affects perfusion of an artificial microvascular network (AMVN).

STUDY DESIGN AND METHODS—Blood samples were obtained from healthy consenting volunteers. RBCs were leukocyte-reduced, re-suspended in saline, and treated with various concentrations of sodium salicylate to induce shape changes approximating the stages of echinocytosis experienced by RBCs during hypothermic storage (e.g. discocyte, echinocyte I, echinocyte II, echinocyte III, sphero-echinocyte and spherocyte). The AMVN perfusion rate was measured for 40% hematocrit suspensions of RBCs with different shapes.

RESULTS—The AMVN perfusion rates for RBCs with discocyte and echinocyte I shapes were similar, but there was a statistically significant decline in the AMVN perfusion rate between RBCs with shapes approximating each subsequent stage of echinocytosis. The difference in AMVN perfusion between discocytes and spherocytes (the last stage of the echinocytic transformation) was 34%.

CONCLUSION—The change in shape of RBCs from normal discocytes progressively through various stages of echinocytosis to spherocytes produced a substantial decline in the ability of these cells to perfuse an artificial microvascular network. Echinocytosis induced by hypothermic storage could therefore be responsible for a similarly substantial impairment of deformability previously observed for stored RBCs.

*Corresponding author: University of Houston, Department of Biomedical Engineering, 3605 Cullen Blvd, Houston, TX 77204-5060; phone: +1 (713) 743-5696; fax: +1 (713) 743-0226; sshevkoplyas@uh.edu.

CONFLICT OF INTEREST: All authors declare no conflict of interest.

Introduction

Under resting conditions, the human red blood cell (RBC) assumes the shape of a biconcave disc, called *discocyte*. This unique shape is explained by a state of least total curvature (and thus minimum bending energy) of RBC membrane.[1] The RBC membrane consists of a lipid bilayer with a spectrin-based membrane cytoskeleton underneath. When either the structural properties of the cytoskeleton or the equilibrium between the two hemi-leaflets of the lipid bilayer are disturbed, the normal discocyte morphology is lost.[2] Genetic defects with membrane protein abnormalities lead to spherocytosis or elliptocytosis.[3] Disturbances in the lipid bilayer lead to stomatocytosis when the inner half of the bilayer is expanded relative to the outer half, and to echinocytosis or RBC crenation when the outer half is expanded relative to the inner half.[4] Lipid bilayer disturbances may occur when certain molecules or drugs intercalate either into the inner or outer hemi-leaflet.[1]

The most common type of RBC shape transformation is *echinocytosis*, which has been observed under various circumstances *in vitro* and *in vivo*. Certain drugs may induce echinocytosis: radiocontrast media,[5,6] propofol,[7] fish oil,[8] 5-fluorouracil,[9] antiepileptic drugs,[10,11] non-steroidal anti-inflammatory drugs[12] and particularly sodium-salicylate (SA), which has been used extensively to study echinocytosis *in vitro*.[13-15] Hemodialysis[16] and extracorporeal circulation during open heart surgery[17] induce some degree of echinocytosis as well. Perhaps the most important instance of echinocytosis occurs during hypothermic storage of RBCs.[18-20] The morphology of stored RBCs progressively deteriorates due to oxidative damage, biochemical changes and microvesiculation.[21-25] Microvesiculation results in a disproportionately larger loss of cell membrane than cell volume, increasing sphericity of the cell. Stored RBCs gradually transition from normal, biconcave discocytes, through distinct intermediate echinocytic stages (echinocyte I, echinocyte II, echinocyte III, sphero-echinocyte) to spherocytes and ultimately undergo lysis.[26] The rate and degree of this morphological deterioration varies greatly between individual RBCs, resulting in a highly heterogeneous population of cells with different morphologies within each stored RBC unit.

It is well known that hypothermic storage impairs RBC deformability, as evidenced by the increasing suspension viscosities[19,20] as well as decreasing ability of stored RBCs to perfuse an artificial microvascular network.[20] It is however not yet known whether RBC *shape* directly and independently affects microvascular perfusion. In this study we investigated the impact of various degrees of echinocytosis (induced by increasing concentrations of sodium salicylate) on perfusion of an artificial microvascular network (AMVN).

Materials and Methods

Device Preparation

A master silicon wafer containing the pattern of the AMVN device was fabricated using soft lithography as described previously.[27-30] The AMVN device consisted of three parallel identical microchannel networks, each with a separate domed inlet port and all converging to the same domed outlet port.[27] The AMVN comprised a system of microchannels with a depth of 5 μm and range of widths from 5 μm to 70 μm connected in a pattern inspired by

the layout of the microvasculature of rat mesentery.[30] Polydimethylsiloxane (PDMS, Sylgard 184, Dow Corning Corp., Midland, MI) was poured over the wafer and cured at 65°C for 3 hours to create a cast of the device. Biopsy punches (Acuderm, Inc., Fort Lauderdale, FL) were used to create access ports for the inlets (4 mm) and outlet (1.5 mm) through the PDMS cast. The AMVN device and a glass slide (VWR, West Chester, PA) spin-coated with a ~50 μm layer of PDMS were then plasma oxidized (100 seconds, air plasma) and bonded to one another. The assembled devices were filled with a 1% solution of mPEG-silane (Laysan Bio, Inc., Arab, AL) in GASP buffer (1.3 mM NaH_2PO_4, 9 mM Na_2HPO_4, 140 mM NaCl, 5.5 mM glucose, 1% bovine serum albumin; osmolality 290 mmol/kg; pH 7.4)[27] and incubated at ambient temperature for at least 8 hours to prevent cell adhesion to the walls of the microchannels. The mPEG-silane solution was flushed from the microchannel with GASP buffer prior to performing experiments.

Sample Preparation

Whole blood was collected from healthy consenting volunteers (n = 5) via venipuncture into Vacutainer tubes containing K_2EDTA anticoagulant (BD, Franklin Lakes, NJ). Blood samples were leukoreduced using a high-efficiency pediatric leukocyte reduction filter (Purecell NEO, Pall Corp., Port Washington, USA).[29] Samples were adjusted to 40% hematocrit (Hct) with normal saline (osmolality 290 mOsm/kg). To create RBC samples with various induced morphologies, 1 mL aliquots of leukoreduced, 40% Hct samples were centrifuged at 2500 × g for 5 minutes at ambient temperature (Microfuge 22R, Beckman Coulter, Fullerton, CA) to separate RBCs from the supernatant. Various volumes of supernatant were removed from the aliquoted samples and replaced with equal amounts of an isotonic stock solution of sodium salicylate (SA) in saline (290 mOsm/kg), to create solutions with final SA concentrations of 0, 9, 18, 27, 36 and 54 mM.[14] The samples were mixed by inversion on a sample tube rotator (Labquake, Barnstead Thermolyne, Dubuque, IA) for 30 minutes prior to use. For each sample, RBC count and mean corpuscular hemoglobin (MCH) were measured with a hematology analyzer (Medonic M-series, Boule Medical AB, Stockholm, Sweden). Hct was measured from the relative fractions of packed RBCs and plasma in untreated plastic 75 mm microcapillary tubes (n = 4; Fisherbrand, Thermo Fisher Scientific, Waltham, MA) centrifuged for 15 minutes at 11,500 × g in a micro-hematocrit centrifuge (PowerSpin BX, UNICO, Princeton, NJ). Hct, measured by microcentrifugation, was used to calculate mean corpuscular volume, MCV = Hct × 10/RBC count. This calculated MCV was then used to calculate mean corpuscular hemoglobin concentration, MCHC = 100 × MCH/MCV.

Imaging and Analysis

An inverted bright-field microscope (IX71, Olympus America Inc., Center Valley, PA, USA) equipped with a high-speed camera (MC1362, Mikrotron GmbH, Unterschleissheim, Germany) was used to acquire images of the post-AMVN (venous) channels at 20x magnification. A band-pass blue-violet filter (394 ± 50 nm, B-390, Hoya Corp. USA, Fremont, CA) was placed between the microscope lamp and condenser in order to improve contrast (RBCs appear dark in blue light). A custom image capture application implemented in Microsoft Visual Studio (Microsoft Corp., Redmond, WA) was used to capture bursts of 10 frames at 100 fps every 10 seconds for the duration of 5 minutes. A custom image

analysis algorithm implemented in MATLAB (The Math Works Inc., Natick, MA, USA) was used to analyze the image sequences and calculate the RBC velocity (V_{RBC}; μm/s) in the channels at each time point based on the shift in RBC position between images. Perfusion rate was defined as the product of the cross sectional area of the post-AMVN microchannel ($A_{channel}$; 350 μm^2) and the measured RBC velocity (perfusion rate = $V_{RBC} \times A_{channel}$; $\mu m^3/s = 1 \times 10^{-6}$ nL/s). For each sample, the perfusion rate was normalized with respect to the perfusion rate of a control sample (normal, untreated RBCs) run through the same device.

Experimental Setup

Figure 1 demonstrates the components of the AMVN measurement system. A water reservoir fixed to a vertical linear motion stage (Series A40 UniSlides, Velmex Inc., Bloomfield, NY) connected with flexible plastic tubing (Tygon R-3603, VWR, West Chester, PA) and a barbed tube fitting (L420/410-6, Value Plastics, Fort Collins, CO) to the outlet of the AMVN device (Figure 1a,b), was used to control the driving pressure of the system by adjusting hydrostatic pressure between the AMVN inlets and the reservoir.[29,30] The microscope field-of-view was then aligned with the post-AMVN venule microchannels and a best-effort manual focusing was performed using the walls of the microchannels as high-contrast standard. To perform the measurement, GASP buffer was removed from the inlets of the AMVN device and 25 μL of RBC sample was deposited in each inlet. The system driving pressure was then set to approximately −10 cmH_2O and the RBCs were allowed to perfuse the system until RBCs from all three inlets reached the outlet port. The water column was then adjusted such that flow through the device stopped (0 cmH_2O driving pressure) and the image capture application was initiated. A baseline perfusion rate (~0 nL/s) was established for 30 seconds, and then the driving pressure was set to −20 cmH_2O for the remainder of the 5 minute image capture period.

The AMVN device consisted of three identical networks of microchannels, each with their own inlet port, converging to the same outlet port (Fig. 1c). Three samples (two experimental and one control) were run in parallel through identical networks within each device. The variation in AMVN perfusion rate between microchannels within a single device is <1%, and the variation between microchannels in different devices is <2%, as previously shown.[27] Samples treated with appropriate concentration of SA to induce each distinct RBC morphology were run in multiple channels within a single device, and in multiple separate devices to minimize potential bias due to minor fabrication irregularities.

Statistical Analysis

Statistical analysis was performed using built-in functions of MATLAB 2014b Statistics Toolbox (The Math Works Inc, Natick, MA). A paired t-test was used for the comparison between two groups. The results are presented as mean values ± standard deviation. A p-value of < 0.01 was considered statistically significant.

Results

Figure 2 illustrates the changes in RBC morphology induced by exposure to different SA concentrations. The specific concentrations of SA were chosen so that the resulting morphologies approximated different degrees of echinocytosis,[26,31] namely: echinocyte I (an irregularly contoured discocyte with up to 5 protrusions) for 9 mM SA; echinocyte II (a flat RBC with a few spicules) for 18 mM SA; echinocyte III (an ovaloid or spherical RBC with many spicules) for 27 mM SA; sphero-echinocyte (a spherical RBC with multiple short and thin spicules) for 36 mM SA; and finally spherocyte (a completely spherical RBC) for 54 mM SA.

Figure 3 shows the characteristic images of RBCs (Fig. 3b) with each of the induced morphologies as they perfused the arteriole and capillary portions of the AMVN (Fig. 3a). Our visual phenomenological observations showed that morphology of RBCs influenced their flow, packing and deformation characteristics within the AMVN. Echinocytic RBCs were unable to form the characteristic bullet shapes as they traversed microcapillaries (Fig. 3b). The spherical geometry of sphero-echinocytes and spherocytes severely limited the number of RBCs which could simultaneously pass through individual microchannels (Fig. 3b).

Figure 4 shows the normalized AMVN perfusion rates for RBCs with different shapes. For each trial, a control, untreated RBC sample (0 mM SA; Hct = 39.6 ± 0.8 %; MCV = 85.6 ± 1.7 fL; MCHC = 32.2 ± 0.6 g/dL) and two experimental, treated RBC samples were analyzed using the three identical channels comprising each AMVN device. RBC samples from each of the five volunteers were used to evaluate each SA concentration independently (50 experiments for untreated samples, 0 mM; n = 19 experiments for each of the samples exposed to 9, 18, 27, 36, and 54 mM of sodium salicylate). The AMVN perfusion rate decreased as the degree of echinocytosis increased. There was only a minor, non-significant decrease in perfusion rate from discocyte to induced echinocyte I (0.1% of discocyte; p = 0.837). The perfusion rate then drastically decreased from echinocyte I to echinocyte II (8.8% of discocyte; p = 0.0000414), more so from echinocyte II to echinocyte III (15.9% of discocyte; p = 0.00000000495), and even further from echinocyte III to sphero-echinocyte (5.8% of discocyte; p = 0.000580). The decrease in the AMVN perfusion rate from sphero-echinocyte to spherocyte (3.0% of discocyte; p = 0.00690) was noticeable but less drastic. Overall, there was a decrease in the AMVN perfusion rate of 33.6% as the RBC shape progressively changed from discocyte to spherocyte (Fig. 4). For context, a previous study found that the overall decrease in AMVN perfusion rate for hypothermically stored RBC units between week 0 and week 6 of storage is approximately 20 – 25%.[20,27]

We found that exposure to SA resulted in small decrease of MCV (up to 5.2 fL) and a modest increase of MCHC (up to 2.0 g/dL) compared to normal discocytes (Table 1), which is in agreement with earlier observations.[14] The decrease in MCV (1.7% of discocyte; p = 0.252) and increase in MCHC (5.0% of discocyte; p = 0.0105) between discocytes (0 mM SA) and induced spherocytes (54 mM SA) were not statistically significant. The decrease in Hct between discocytes and induced spherocytes, potentially due to lysis, was statistically significant (5.7% of discocyte; p = 0.00499). For all of our samples, MCHC ranged from

32.0 to 34.0 g/dL, and the maximum decrease in AMVN perfusion rate was 0.084 nL/s (or 33.6% of the perfusion rate for discocytes). We have previously shown that changes in MCHC of up to 7.8 g/dL produce a decrease in the AMVN perfusion rate of <0.016 nL/s (or 6.6% of discocyte).[32] The decreases in AMVN perfusion rate experienced by induced echinocyte II (9.0% of discocyte), echinocyte III (24.9% of discocyte), sphero-echinocytes (30.6% of discocyte) and spherocytes (33.6% of discocyte) were all significantly greater than would be expected based on change in MCHC alone.

Discussion

SA produced a concentration-dependent echinocytic shape transformation comparable to earlier studies.[13-15,33-35] The influence of SA-induced echinocytosis on rheological parameters has been extensively studied in the past. RBC suspension viscosity is increased, due to mechanical hindrance between spiculated RBCs.[13,14,34] RBC aggregation is drastically reduced because spiculated RBCs are unable to make large enough surface area contact with neighboring cells to form stable aggregates.[33,34] The passage of narrow filter pores with a nominal diameter of 3μm (i.e. smaller than the diameter of the smallest capillary in our AMVN device) was not hindered, but even facilitated by SA-induced echinocytosis of higher degree, explained by a preserved or even increased surface area to volume ratio of echinocytes, which is the most relevant parameter for the passage of very narrow pores.[14] On the level of membrane deformability, micropipette experiments have shown that echinocytes induced by SA had a slightly increased resistance to membrane extension.[35] Shape normalization by the addition of a counteracting stomatocytogenic agent such as chlorpromazine normalized these rheological alterations, indicating that the shape matters and not the drug interaction with the RBC membrane itself.[34,35] Taken together, these divergent rheological results make it difficult to anticipate the role of the RBC shape in microvascular perfusion, which is most important in (patho)physiological and clinical terms and has prompted the present study.

We found that perfusion of the artificial microvascular network (AMVN) was maximized for RBCs of normal biconcave discoid and echinocyte I shape. These results suggest that although discocytes are best for microvascular perfusion, some degree of RBC shape deterioration such as the initial stages of echinocytosis could be well-tolerated by the microvasculature. Further progression of RBCs along the path of the echinocytic transformation towards spherocytosis gradually decreased the AMVN perfusion in our experiments. The maximum average drop of the AMVN perfusion rate we measured in this study was approximately 30% for the sample that mostly consisted of spherocytes (the end point of the echinocytic transformation). Echinocytosis is by far the most common type of RBC shape deterioration occurring during hypothermic storage,[26] and therefore our results could have particularly important implications in the context of blood storage and transfusion. Interestingly, in our previous studies we measured a 20-25% difference in the AMVN perfusion rate between fresh RBC (mostly discocytes) and RBC stored hypothermically for 6 weeks.[20,27] Because 6-week old blood is a heterogeneous mixture composed predominantly of cells in early stages of echinocytosis (which may recover their shape *in vivo*, post-transfusion[36] or via washing[20]), some discocytes and a sizable fraction of irreparably damaged late stage echinocytes and spherocytes,[26] the shape change could

explain a large fraction of the decline in the AMVN perfusion rate we have previously measured for hypothermically stored blood.

During flow in the circulation, RBCs are exposed to a large variety of shear stresses, ranging from very small, such as in the axis of a large vessel, where the shear stress approaches zero, to very large shear stresses, such as in capillaries, where the strongest RBC deformation occurs. The deformation into a bullet-like shape in smaller capillaries is only possible because RBCs have a high surface area to volume ratio, which is a geometric prerequisite for this deformation.[37] When the surface area to volume ratio is decreased (i.e. RBCs become more spherical as seen in hypotonic swelling) RBC deformability in capillaries is reduced, which reduces the AMVN perfusion rate.[32] The present data and earlier observations[14] indicate that echinocytosis induced by SA does not decrease the surface area to volume ratio of RBCs, thus allowing an unhindered passage of smallest capillaries (5 μm) within the AMVN (or even narrower channels such as 3 μm filter pores[14]) despite the fact that echinocytes have an increased resistance to membrane deformation as measured by the micropipette aspiration technique,[35] and an increased suspension viscosity due to the entanglement among spiculated RBCs.[14,19] We conclude, therefore, that the decrease in the ability of echinocytic RBCs to perfuse the AMVN was not caused by a deformability-dependent reduced capacity of single RBCs to pass through the smallest capillaries, but was caused primarily by an impaired flow in arteriole/venule-sized channels (13-70 μm).

Our present data suggest that deterioration of RBC shape occurring during hypothermic storage is likely a significant cause of the storage-induced decline of RBC deformability, particularly as reflected by a reduction in the ability of stored RBCs to perfuse an artificial microvascular network. It has been shown that RBC units stored for less than 2 weeks (and therefore containing on average less echinocytes[19]) decrease post-transfusion morbidity and mortality in patients undergoing cardiac surgery,[38,39] which has, however, not been confirmed by a more recent study.[40] Our data suggest that the degree of storage-induced echinocytosis in each particular RBC unit could influence microcirculatory blood flow *in vivo* and thus contribute to different clinical outcomes.[41] We had previously shown that severe echinocytosis after prolonged hypothermic storage can be partially reversed towards discocytosis by washing stored RBCs in a 1% human serum albumin (HSA) solution, a procedure that also significantly improves the ability of stored RBCs to perfuse the AMVN.[20] We reason therefore that if the echinocytic transformation of RBC shape due to hypothermic storage could be either completely prevented, or arrested in its earliest stages (e.g. echinocyte I), or reversed through some kind of treatment right before transfusion (e.g. washing in 1% HSA) the microvascular perfusion in the recipient may be improved.

Our results may have important implications in other clinically-relevant contexts. For example, it is well-known that radiographic contrast media may induce echinocytosis *in vivo*.[42] Angiography (e.g. of the brain, heart, or leg) may induce echinocytosis, which could, at least temporarily, reduce microvascular perfusion and by doing so deteriorate critical peripheral ischemia further. It is, therefore, advisable to use the smallest possible volume of contrast medium and choose one with low echinocytogenic properties.[5,42] Although our results cannot be easily generalized for other, similar shape abnormalities (e.g. acanthocytosis[43,44]), it is very likely that they might be disadvantageous as well.

We conclude that normal discocytes represent the optimum RBC shape for AMVN perfusion and that the echinocytic shape transformation leads to a progressive decrease of AMVN perfusion rates. RBC shape is an indicator of the rheological performance of RBCs in the microvasculature and therefore could be used as a measure of the quality of stored blood units.

Acknowledgments

SOURCE OF SUPPORT: This work was supported by a 2012 NIH Director's Transformative Research Award (NHLBI R01HL117329, PI: Shevkoplyas).

References

1. Canham PB. The minimum energy of bending as a possible explanation of the biconcave shape of the human red blood cell. J Theor Biol. 1970; 26:61–81. [PubMed: 5411112]
2. Reinhart WH. Peculiar red cell shapes: Fahraeus Lecture 2011. Clin Hemorheol Microcirc. 2011; 49:11–27. [PubMed: 22214674]
3. de Oliveira S, Saldanha C. An overview about erythrocyte membrane. Clin Hemorheol Microcirc. 2010; 44:63–74. [PubMed: 20134094]
4. Sheetz MP, Singer SJ. Biological membranes as bilayer couples. A molecular mechanism of drug-erythrocyte interactions. Proc Natl Acad Sci U S A. 1974; 71:4457–61. [PubMed: 4530994]
5. Reinhart WH, Pleisch B, Harris LG, Lutolf M. Influence of contrast media (iopromide, ioxaglate, gadolinium-DOTA) on blood viscosity, erythrocyte morphology and platelet function. Clin Hemorheol Microcirc. 2005; 32:227–39. [PubMed: 15851842]
6. Mrowietz C, Franke RP, Jung F. Influence of different radiographic contrast media on the echinocyte formation of human erythrocytes. Clin Hemorheol Microcirc. 2012; 50:35–47. [PubMed: 22538533]
7. Reinhart WH, Felix C. Influence of propofol on erythrocyte morphology, blood viscosity and platelet function. Clin Hemorheol Microcirc. 2003; 29:33–40. [PubMed: 14561902]
8. Fischler L, Meredith DO, Reinhart WH. Influence of a parenteral fish-oil preparation (Omegaven) on erythrocyte morphology and blood viscosity in vitro. Clin Hemorheol Microcirc. 2003; 28:79–88. [PubMed: 12652013]
9. Baerlocher GM, Beer JH, Owen GR, Meiselman HJ, Reinhart WH. The anti-neoplastic drug 5-fluorouracil produces echinocytosis and affects blood rheology. Br J Haematol. 1997; 99:426–32. [PubMed: 9375767]
10. Suwalsky M, Mennickent S, Norris B, Villena F, Sotomayor CP. Effects of the antiepileptic drug carbamazepine on human erythrocytes. Toxicol In Vitro. 2006; 20:1363–9. [PubMed: 16844339]
11. Reinhart WH, Lubszky S, Thony S, Schulzki T. Interaction of injectable neurotropic drugs with the red cell membrane. Toxicol In Vitro. 2014; 28:1274–9. [PubMed: 24997296]
12. Manrique-Moreno M, Suwalsky M, Villena F, Garidel P. Effects of the nonsteroidal anti-inflammatory drug naproxen on human erythrocytes and on cell membrane molecular models. Biophys Chem. 2010; 147:53–8. [PubMed: 20083338]
13. Meiselman HJ. Rheology of shape-transformed human red cells. Biorheology. 1978; 15:225–37. [PubMed: 737324]
14. Reinhart WH, Chien S. Red cell rheology in stomatocyte-echinocyte transformation: roles of cell geometry and cell shape. Blood. 1986; 67:1110–8. [PubMed: 3955230]
15. Li A, Seipelt H, Muller C, Shi Y, Artmann M. Effects of salicylic acid derivatives on red blood cell membranes. Pharmacol Toxicol. 1999; 85:206–11. [PubMed: 10608482]
16. Hasler CR, Owen GR, Brunner W, Reinhart WH. Echinocytosis induced by haemodialysis. Nephrol Dial Transplant. 1998; 13:3132–7. [PubMed: 9870478]
17. Reinhart WH, Ballmer PE, Rohner F, Ott P, Straub PW. The influence of extracorporeal circulation on erythrocytes and flow properties of blood. J Thorac Cardiovasc Surg. 1990; 100:538–45. [PubMed: 2145479]

18. Relevy H, Koshkaryev A, Manny N, Yedgar S, Barshtein G. Blood banking-induced alteration of red blood cell flow properties. Transfusion. 2008; 48:136–46. [PubMed: 17900281]
19. Zehnder L, Schulzki T, Goede JS, Hayes J, Reinhart WH. Erythrocyte storage in hypertonic (SAGM) or isotonic (PAGGSM) conservation medium: influence on cell properties. Vox Sang. 2008; 95:280–7. [PubMed: 19138257]
20. Reinhart WH, Piety NZ, Deuel JW, Makhro A, Schulzki T, Bogdanov N, Goede JS, Bogdanova A, Abidi R, Shevkoplyas SS. Washing stored red blood cells in an albumin solution improves their morphologic and hemorheologic properties. Transfusion. 2015
21. Kim-Shapiro DB, Lee J, Gladwin MT. Storage lesion: role of red blood cell breakdown. Transfusion. 2011; 51:844–51. [PubMed: 21496045]
22. Karon BS, van Buskirk CM, Jaben EA, Hoyer JD, Thomas DD. Temporal sequence of major biochemical events during blood bank storage of packed red blood cells. Blood Transfus. 2012; 10:453–61. [PubMed: 22507860]
23. Rinalducci S, Ferru E, Blasi B, Turrini F, Zolla L. Oxidative stress and caspase-mediated fragmentation of cytoplasmic domain of erythrocyte band 3 during blood storage. Blood Transfus. 2012; 10(Suppl 2):s55–62. [PubMed: 22890269]
24. Almizraq R, Tchir JD, Holovati JL, Acker JP. Storage of red blood cells affects membrane composition, microvesiculation, and in vitro quality. Transfusion. 2013; 53:2258–67. [PubMed: 23320518]
25. Hess JR. Red cell changes during storage. Transfus Apher Sci. 2010; 43:51–9. [PubMed: 20558107]
26. Piety NZ, Gifford SC, Yang X, Shevkoplyas SS. Quantifying morphological heterogeneity: a study of more than 1 000 000 individual stored red blood cells. Vox Sang. 2015
27. Burns JM, Yang X, Forouzan O, Sosa JM, Shevkoplyas SS. Artificial microvascular network: a new tool for measuring rheologic properties of stored red blood cells. Transfusion. 2012; 52:1010–23. [PubMed: 22043858]
28. Sosa JM, Nielsen ND, Vignes SM, Chen TG, Shevkoplyas SS. The relationship between red blood cell deformability metrics and perfusion of an artificial microvascular network. Clin Hemorheol Microcirc. 2014; 57:275–89. [PubMed: 23603326]
29. Forouzan O, Yang X, Sosa JM, Burns JM, Shevkoplyas SS. Spontaneous oscillations of capillary blood flow in artificial microvascular networks. Microvasc Res. 2012; 84:123–32. [PubMed: 22732344]
30. Shevkoplyas SS, Yoshida T, Gifford SC, Bitensky MW. Direct measurement of the impact of impaired erythrocyte deformability on microvascular network perfusion in a microfluidic device. Lab Chip. 2006; 6:914–20. [PubMed: 16804596]
31. Bessis M. Red cell shapes. An illustrated classification and its rationale. Nouv Rev Fr Hematol. 1972; 12:721–45. [PubMed: 4268780]
32. Reinhart WH, Piety NZ, Goede JS, Shevkoplyas SS. Effect of osmolality on erythrocyte rheology and perfusion of an artificial microvascular network. Microvasc Res. 2015; 98:102–7. [PubMed: 25660474]
33. Reinhart WH, Singh A, Straub PW. Red blood cell aggregation and sedimentation: the role of the cell shape. Br J Haematol. 1989; 73:551–6. [PubMed: 2611140]
34. Reinhart WH, Singh-Marchetti M, Straub PW. The influence of erythrocyte shape on suspension viscosities. Eur J Clin Invest. 1992; 22:38–44. [PubMed: 1559541]
35. Chabanel A, Reinhart W, Chien S. Increased resistance to membrane deformation of shape-transformed human red blood cells. Blood. 1987; 69:739–43. [PubMed: 3814814]
36. Rumsby MG, Trotter J, Allan D, Michell RH. Recovery of membrane micro-vesicles from human erythrocytes stored for transfusion: a mechanism for the erythrocyte discocyte-to-spherocyte shape transformation. Biochem Soc Trans. 1977; 5:126–8. [PubMed: 892138]
37. Kowluru R, Bitensky MW, Kowluru A, Dembo M, Keaton PA, Buican T. Reversible sodium pump defect and swelling in the diabetic rat erythrocyte: effects on filterability and implications for microangiopathy. Proc Natl Acad Sci U S A. 1989; 86:3327–31. [PubMed: 2541440]

38. Koch CG, Li L, Sessler DI, Figueroa P, Hoeltge GA, Mihaljevic T, Blackstone EH. Duration of red-cell storage and complications after cardiac surgery. N Engl J Med. 2008; 358:1229–39. [PubMed: 18354101]

39. Redlin M, Habazettl H, Schoenfeld H, Kukucka M, Boettcher W, Kuppe H, Salama A. Red blood cell storage duration is associated with various clinical outcomes in pediatric cardiac surgery. Transfus Med Hemother. 2014; 41:146–51. [PubMed: 24847191]

40. Steiner ME, Ness PM, Assmann SF, Triulzi DJ, Sloan SR, Delaney M, Granger S, Bennett-Guerrero E, Blajchman MA, Scavo V, Carson JL, Levy JH, Whitman G, D'Andrea P, Pulkrabek S, Ortel TL, Bornikova L, Raife T, Puca KE, Kaufman RM, Nuttall GA, Young PP, Youssef S, Engelman R, Greilich PE, Miles R, Josephson CD, Bracey A, Cooke R, McCullough J, Hunsaker R, Uhl L, McFarland JG, Park Y, Cushing MM, Klodell CT, Karanam R, Roberts PR, Dyke C, Hod EA, Stowell CP. Effects of red-cell storage duration on patients undergoing cardiac surgery. N Engl J Med. 2015; 372:1419–29. [PubMed: 25853746]

41. Somani A, Steiner ME, Hebbel RP. The dynamic regulation of microcirculatory conduit function: features relevant to transfusion medicine. Transfus Apher Sci. 2010; 43:61–8. [PubMed: 20580315]

42. Franke RP, Kruger A, Scharnweber T, Wenzel F, Jung F. Effects of radiographic contrast media on the micromorphology of the junctional complex of erythrocytes visualized by immunocytology. Int J Mol Sci. 2014; 15:16134–52. [PubMed: 25222553]

43. Lange Y, Steck TL. Mechanism of red blood cell acanthocytosis and echinocytosis in vivo. J Membr Biol. 1984; 77:153–9. [PubMed: 6708089]

44. De Franceschi L, Bosman GJ, Mohandas N. Abnormal red cell features associated with hereditary neurodegenerative disorders: the neuroacanthocytosis syndromes. Curr Opin Hematol. 2014; 21:201–9. [PubMed: 24626044]

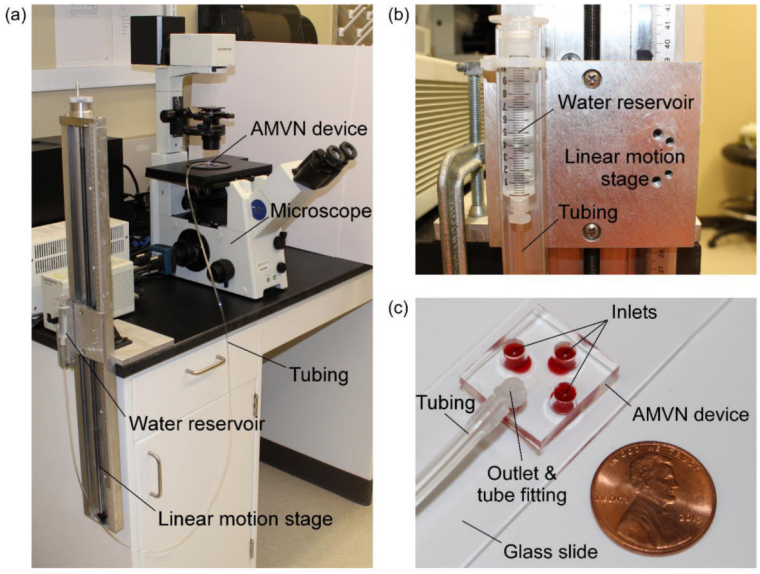

Fig. 1.

Representative images of RBCs treated with various concentrations of sodium salicylate (SA). Exposure to SA changed the shape of RBCs in a dose-dependent fashion, approximating the increasing degrees of echinocytosis (0 mM – discocyte; 9 mM – echinocyte I; 18 mM – echinocyte II; 27 mM – echinocyte III; 36 mM – sphero-echinocyte, 54 mM – spherocyte). Scale bar is 10 μm.

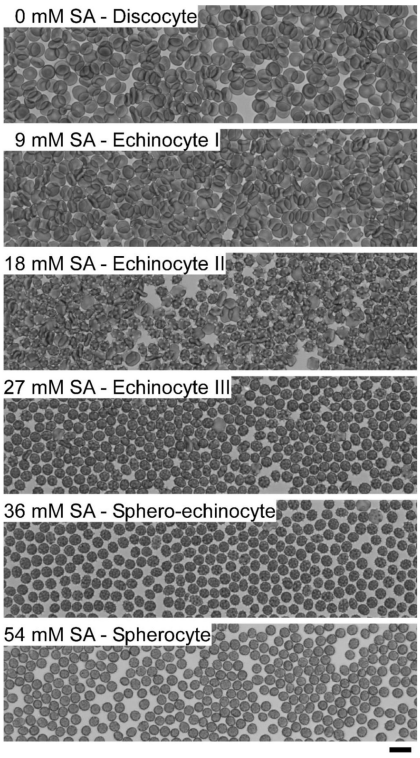

Fig. 2.

Setup for measuring the AMVN perfusion rate. (**a**) Complete AMVN system. (**b**) A reservoir attached to the vertical linear motion stage is used to control the driving pressure of the AMVN system. The AMVN device is connected to the reservoir by a length of plastic tubing through a barbed tube fitting. (**c**) Photograph of the AMVN device loaded with an RBC sample (one-cent U.S. coin is shown for size reference).

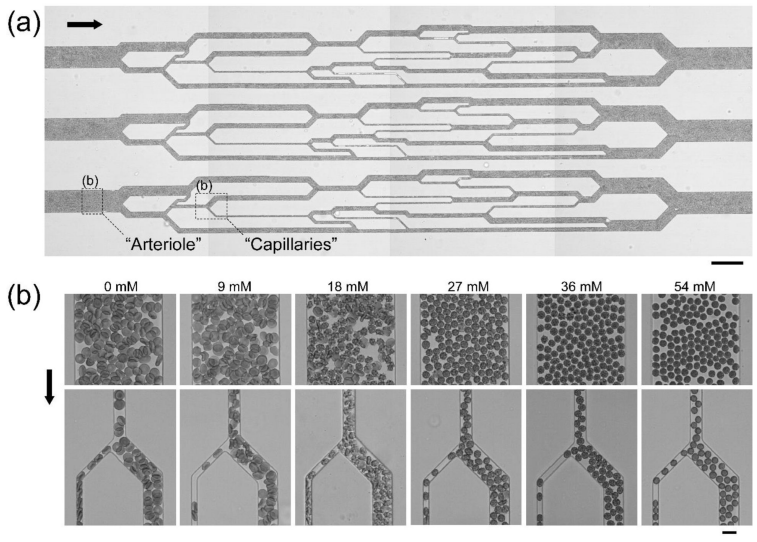

Fig. 3.

The flow patterns of blood samples with RBCs of different shapes in the AMVN. (**a**) Bright-field micrograph of the three parallel microvascular network units of the AMVN device containing RBCs (arrow indicates direction of flow, scale bar is 100 μm). (**b**) Bright-field micrographs of RBCs exposed to various concentrations of sodium salicylate as they perfuse portions of the AMVN: (**upper row**) 70 μm AMVN arteriole microchannel; (**lower row**) 10 μm capillary microchannel splitting into a 5 μm and a 15 μm capillary microchannels (arrow indicates direction of flow, scale bar is 10 μm).

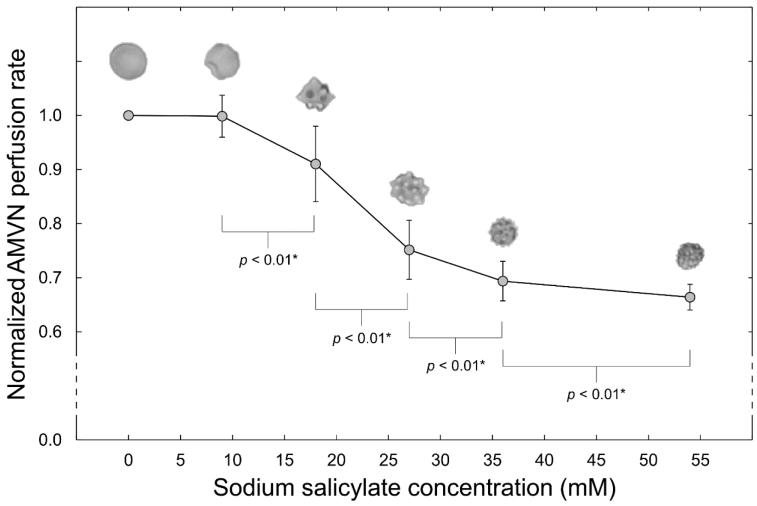

Fig. 4.

The dependence of the AMVN perfusion rate on RBC shape. Inset images show (from left to right) a discocyte, an echinocyte I, an echinocyte II, an echinocyte III, a sphero-echinocyte, and a spherocyte. Perfusion rates were normalized with respect to the perfusion rate of normal RBCs (discocytes; 0 mM SA). Mean values ± standard deviation; 50 experiments for untreated samples, 0 mM; 19 experiments for each of the samples exposed to 9, 18, 27, 36, and 54 mM of sodium salicylate. The *p*-values indicate the statistical significance of the change in mean AMVN perfusion rate between the bracketed RBC shapes (asterisk denotes a significant change).

Table 1

Summary of hemorheological parameters at different sodium salicylate concentrations (mean values ± standard deviation, n = 5). Hct was measured by microcentrifugation. RBC number was measured by hematology analyzer. Mean corpuscular volume was calculated as MCV = Hct × 10/RBC count, where RBC count was measured by hematology analyzer. Mean corpuscular hemoglobin concentration was calculated as MCHC = 100 × MCH/MCV, where MCH (mean corpuscular hemoglobin) was measured by hematology analyzer. Measured non-normalized AMVN perfusion rate (mean values ± standard deviation; 50 experiments for untreated samples, 0 mM; 19 experiments for each of the samples exposed to 9, 18, 27, 36, and 54 mM of sodium salicylate).

	Sodium salicylate concentration (mM)					
	0	**9**	**18**	**27**	**36**	**54**
Hct (%)	39.6 ± 0.8	39.7 ± 0.9	38.9 ± 0.3	39.0 ± 0.6	38.8 ± 0.6	37.4 ± 0.5
RBC count (10^{12}/L)	4.63 ± 0.00	4.58 ± 0.00	4.63 ± 0.00	4.79 ± 0.00	4.64 ± 0.00	4.44 ± 0.00
MCV (fL)	85.6 ± 1.7	86.6 ± 2.0	84.0 ± 0.7	81.4 ± 1.3	83.7 ± 1.4	84.2 ± 1.0
MCHC (g/dL)	32.2 ± 0.6	32.0 ± 0.7	33.0 ± 0.3	34.0 ± 0.5	33.8 ± 0.5	33.9 ± 0.4
AMVN perfusion rate (nL/s)	0.268 ± 0.022	0.261 ± 0.025	0.237 ± 0.021	0.198 ± 0.012	0.187 ± 0.011	0.182 ± 0.012